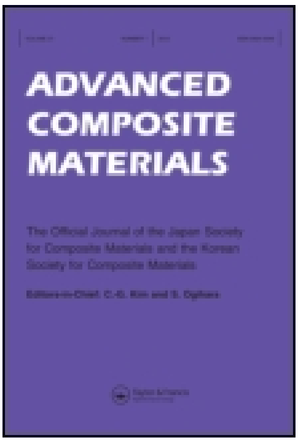

Advanced Composite Materials
Publication details, including instructions for authors and subscription information:
http://www.tandfonline.com/loi/tacm20

Modeling creep and recovery behavior of a quasi-isotropic laminate with transverse cracking

Keiji Ogi & P. A. Smith

Version of record first published: 02 Apr 2012.

Adv. Composite Mater., Vol. 11, No. 1, pp. 81–93 (2002)

Modeling creep and recovery behavior of a quasi-isotropic laminate with transverse cracking

KEIJI OGI [1,*] and P. A. SMITH [2]

[1] *Faculty of Engineering, Ehime University, 3 Bunkyocho, Matsuyama, Ehime, 790-8577, Japan*
[2] *School of Mechanical and Materials Engineering, University of Surrey, Guildford, Surrey, GU2 5XH, UK*

Abstract—An analytical model is proposed for predicting creep and recovery behavior of a quasi-isotropic laminate having transverse cracks in transverse layers. The analysis is established on the basis of a shear lag analysis in conjunction with a viscoelasticity theory. The strain is obtained in the Laplace transformed space and its original function is calculated by means of a numerical inverse Laplace transform technique. Creep and recovery tests are conducted for a quasi-isotropic glass/epoxy (GFRP) laminate with and without transverse cracking at a room temperature. The predicted strain response is in reasonably good agreement with experimental results.

Keywords: Transverse cracking; quasi-isotropic laminate; shear lag analysis; viscoelasticity; creep; recovery.

1. INTRODUCTION

While much analytical and experimental work has been done on the damage mechanism of composites, time-dependent behavior of damaged composites has received little attention in the literature. Some experimental work [1, 2] has been conducted on time-dependent transverse cracking of cross-ply laminates. Moore and Dillard [1] investigated time-dependent cumulative matrix cracking in graphite/epoxy and Kevlar/epoxy laminates. Raghavan and Meshii [2] conducted constant strain rate and constant stress tests of AS4/3501-6 cross-ply laminates and showed that the matrix crack density and its rate of increase depend on strain rate and stress, respectively. Recently, Ogi and Takao [3, 4] have developed a shear lag-based model to predict the strain response and transverse crack density in a carbon/epoxy cross-ply laminate under monotonic and constant loading. In their model, a shear lag parameter is assumed to be independent of time. In

*To whom correspondence should be addressed. E-mail: kogi@en2.ehime-u.ac.jp

the subsequent paper [5], a modified model is proposed, in which the shear lag parameter is time-dependent. With regard to an isotropic laminate, Ogi and Smith [6] showed some experimental results on time-dependent behavior of a cracked GFRP laminate loaded in flexure.

In the present study, creep and recovery behavior of a $[0°/90°/-45°/45°]_S$ quasi-isotropic laminate with transverse cracking is presented. The viscoelastic shear lag model is established for a quasi-isotropic laminate with transverse cracking in the transverse layers. Numerical simulation is conducted to predict the strain for creep and recovery of the laminate. Viscoelastic constants required for the simulation are obtained from creep tests of [0°], [10°], [90°] and $[\pm 45°]_S$ specimens. The predictions are compared with experimental results of a quasi-isotropic GFRP laminate with and without transverse cracking to verify the model.

2. MODELING

2.1. Assumptions

Figure 1 illustrates a $[0°/90°/-45°/+45°]_S$ laminate and a coordinate system. The assumptions made for establishing a model are stated below:

(a) The ply group consisting of the $-45°$ and $+45°$ layers behaves as a $[\pm 45°]_S$ laminate [6].
(b) Based on Saint-Venant's principle, the thickness of the shear-deformed region in the 0° and $-45°$ layers is a half of the transverse layer [7].
(c) Parabolic distributions of the displacements in the x-direction are assumed. This leads to the linear distributions of the shear stress τ_{xz} in the shear-deformed region [8].
(d) The displacements in the z-direction are independent of x.
(e) The axial mechanical strain averaged through the thickness in the 0° layer is identical to that in the $[\pm 45°]_S$ laminate.
(f) The thermal strains are independent of time.
(g) Transverse crack density is kept constant during a creep and recovery process.

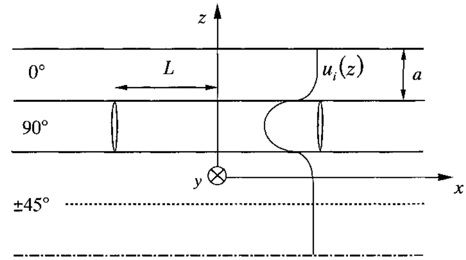

Figure 1. A schematic of a $[0°/90°/-45°/+45°]_S$ quasi-isotropic laminate with transverse cracking and its coordinate system.

2.2. Governing equations

From the assumptions (b) and (c), the displacements $u_k (k = 1, 2, 3)$ in the x directions are expressed as a function of x, z and time t:

$$
\begin{aligned}
u_1(x,z,t) &= \begin{cases} 4C_1a^2 + 2C_2a + C_3 & (2a < z \leqslant 5a/2), \\ C_1z^2 + C_2z + C_3 & (3a/2 < z \leqslant 2a), \end{cases} \\
u_2(x,z,t) &= C_4z^2 + C_5z + C_6 \qquad\qquad (a/2 < z \leqslant 3a/2), \\
u_3(x,z,t) &= \begin{cases} C_7z^2 + C_8z + C_9 & (0 < z \leqslant a/2), \\ C_9 & (-3a/2 \leqslant z \leqslant 0), \end{cases}
\end{aligned} \tag{1}
$$

where the subscript k of 1, 2, and 3 denotes the 0° layer, 90° layer and $[\pm 45°]_S$ laminate, respectively, a denotes the thickness of each layer and $C_i (i = 1, \ldots 9)$ are functions of x and t.

The shear stresses $\tau_{xz,k}$ is expressed as a hereditary integral as

$$\tau_{xz,k}(x,z,t) = G_k(t)\,\gamma_{xz,k}(x,z,0) + \int_0^t G_k(t-\tau)\frac{\partial \gamma_{xz,k}(x,z,\tau)}{\partial \tau}\,\mathrm{d}\tau, \tag{2}$$

where $G_k(t)$ denotes the through-the-thickness shear modulus and $\gamma_{xz,k}(x,z,t)$ is the shear strain expressed by using the assumption (d) as

$$\gamma_{xz,k}(x,z,t) = \frac{\partial u_k(x,z,t)}{\partial z}. \tag{3}$$

On the other hand, the axial strain in each layer is decomposed into the mechanical and thermal components as

$$\varepsilon_k(x,t) = \frac{\partial \bar{u}_k(x,t)}{\partial x} + \varepsilon_k^{\mathrm{T}}, \tag{4}$$

where $\bar{u}_k(x,t)$ denotes the average through-the-thickness displacement and $\varepsilon_k^{\mathrm{T}}$ is the thermal strain having a constant value (assumption (f)). The following relation is derived from the assumption (e):

$$\frac{\partial \bar{u}_1(x,t)}{\partial x} = \frac{\partial \bar{u}_3(x,t)}{\partial x}. \tag{5}$$

The relationship between the axial stress σ_k and strain ε_k in each layer is given by the viscoelastic constitutive equation:

$$\sigma_k(x,t) = E_k(t)\varepsilon_k(x,0) + \int_0^t E_k(t-\tau)\,\frac{\partial \varepsilon_k(x,\tau)}{\partial \tau}\,\mathrm{d}\tau, \tag{6}$$

where $E_k(t)$ denotes the Young's modulus of each layer.

The boundary conditions are

$$\tau_{xz,3} = 0 \qquad \text{at } z = 0, \tag{7.1}$$

$$\tau_{xz,2} = \tau_{xz,3} = \tau_2(x,t) \qquad \text{at } z = a/2, \tag{7.2}$$

$$\tau_{xz,1} = \tau_{xz,2} = \tau_1(x,t) \qquad \text{at } z = 3a/2, \tag{7.3}$$

$$\tau_{xz,1} = 0 \quad \text{at } z = 2a, \tag{7.4}$$
$$u_2 = u_3 \quad \text{at } z = a/2, \tag{7.5}$$
$$u_1 = u_2 \quad \text{at } z = 3a/2, \tag{7.6}$$
$$u_1 = u_2 = u_3 = 0 \quad \text{at } x = 0, \tag{7.7}$$
$$\sigma_2 = 0 \quad \text{at } x = \pm L, \tag{7.8}$$

where τ_1 and τ_2 denote the shear stress at the interfaces between the 0° layer and 90° layer and between the 90° layer and $[\pm 45°]_S$ laminate, respectively.

From the force balance in the laminate and each layer we obtain

$$\sigma_1(x,t) + \sigma_2(x,t) + 2\sigma_3(x,t) = 4\sigma_a(t), \tag{8}$$

$$a\frac{\partial \sigma_1(x,t)}{\partial x} - \tau_1(x,t) = 0, \tag{9.1}$$

$$a\frac{\partial \sigma_2(x,t)}{\partial x} + \tau_1(x,t) - \tau_2(x,t) = 0, \tag{9.2}$$

$$2a\frac{\partial \sigma_3(x,t)}{\partial x} + \tau_2(x,t) = 0, \tag{9.3}$$

where $\sigma_a(t)$ is the applied stress.

2.3. Stress distributions

In order to solve the viscoelastic problem, all the calculations are made in the Laplace transformed space. After some calculations (Appendix 1), we obtain a differential equation with respect to $\hat{\sigma}_2(x,s)$ as

$$\frac{\partial^2 \hat{\sigma}_2(x,s)}{\partial x^2} - \{\hat{\alpha}(s)\}^2 \hat{\sigma}_2(x,s) = -\hat{\beta}(s), \tag{10}$$

with

$$\{\hat{\alpha}(s)\}^2 = \frac{4\,\hat{H}(s)\,\hat{E}_0(s)}{\hat{E}_2(s)\,(4\,\hat{E}_0(s) - \hat{E}_2(s))}, \tag{11}$$

$$\hat{\beta}(s) = \frac{4\,\hat{H}(s)}{4\,\hat{E}_0(s) - \hat{E}_2(s)}\left[\hat{\sigma}_a(s) + \frac{\hat{E}_0(s)}{\hat{E}_2(s)}\,\hat{\sigma}_2^{\mathrm{T}}(s)\right], \tag{12}$$

$$\hat{E}_0(s) = \frac{\hat{E}_1(s) + \hat{E}_2(s) + 2\hat{E}_3(s)}{4}, \tag{13}$$

where $\hat{H}(s)$ is given by equation (A6) and E_0 denotes the Young's modulus of an intact laminate. Using the boundary condition equation (7.8), the solution of equation (10) becomes

$$\hat{\sigma}_2(x,s) = \left\{\frac{\hat{E}_2(s)}{\hat{E}_0(s)}\,\hat{\sigma}_a(s) + \hat{\sigma}_2^{\mathrm{T}}(s)\right\}\left\{1 - \frac{\cosh(\hat{\alpha}(s)\,x)}{\cosh(\hat{\alpha}(s)\,L)}\right\}. \tag{14}$$

Thus, the Laplace transforms of the stresses in the 0° and 90° layers are

$$\hat{\sigma}_1(x,s) = \frac{\hat{E}_1(s)}{\hat{E}_0(s)}\hat{\sigma}_a(s) + \hat{\sigma}_1^{T}(s) + \frac{\hat{E}_1(s)}{4\hat{E}_0(s) - \hat{E}_2(s)}\left\{\frac{\hat{E}_2(s)}{\hat{E}_0(s)}\hat{\sigma}_a(s) + \hat{\sigma}_2^{T}(s)\right\}\frac{\cosh(\hat{\alpha}(s)\,x)}{\cosh(\hat{\alpha}(s)\,L)}, \quad (15)$$

$$\hat{\sigma}_3(x,s) = \frac{\hat{E}_3(s)}{\hat{E}_0(s)}\hat{\sigma}_a(s) + \hat{\sigma}_3^{T}(s) + \frac{\hat{E}_3(s)}{4\hat{E}_0(s) - \hat{E}_2(s)}\left\{\frac{\hat{E}_2(s)}{\hat{E}_0(s)}\hat{\sigma}_a(s) + \hat{\sigma}_2^{T}(s)\right\}\frac{\cosh(\hat{\alpha}(s)\,x)}{\cosh(\hat{\alpha}(s)\,L)}. \quad (16)$$

2.4. Strain response

The Laplace transform of the mean strain of the laminate between two transverse cracks $\bar{\varepsilon}_1(t)$ is calculated as

$$\hat{\bar{\varepsilon}}_1(s) = \frac{1}{L}\int_0^L \frac{\hat{\sigma}_1(x,s)}{s\,\hat{E}_1(s)}\,\mathrm{d}x = \frac{\hat{\sigma}_a(s)}{s\hat{E}_0(s)} + \frac{\hat{\sigma}_1^{T}(s)}{s\hat{E}_1(s)} + \frac{\hat{E}_2(s)}{4\hat{E}_0(s) - \hat{E}_2(s)}\left[\frac{\hat{\sigma}_a(s)}{s\hat{E}_0(s)} + \frac{\hat{\sigma}_2^{T}(s)}{s\hat{E}_2(s)}\right]\frac{\tanh(\hat{\alpha}(s)\,L)}{\hat{\alpha}(s)\,L}. \quad (17)$$

The strain of the laminate ε_L, which is identical to the strain in the 0° layer expressed by equation (17), has the form

$$\hat{\varepsilon}_L(s) = \hat{\varepsilon}_0(s) + \varepsilon_1^{T}/s + \left(s\hat{\varepsilon}_0(s) + \varepsilon_2^{T}\right)\hat{f}(s), \quad (18)$$

with

$$\hat{\varepsilon}_0(s) = \frac{\hat{\sigma}_a(s)}{s\,\hat{E}_0(s)}, \quad (19)$$

$$\hat{f}(s) = \frac{\hat{E}_2(s)}{4\hat{E}_0(s) - \hat{E}_2(s)}\frac{\tanh(\hat{\alpha}(s)\,L)}{s\,\hat{\alpha}(s)\,L}. \quad (20)$$

Inverting equation (18) to the real space, we obtain

$$\varepsilon_L(t) = \varepsilon_L^{M}(t) + \varepsilon_L^{T}(t), \quad (21)$$

with

$$\varepsilon_L^{M}(t) = \varepsilon_0(t) + f(t)\varepsilon_0(0) + \int_0^t f(t-\tau)\frac{\mathrm{d}\varepsilon_0(\tau)}{\mathrm{d}\tau}\,\mathrm{d}\tau, \quad (22.1)$$

$$\varepsilon_L^{T}(t) = \varepsilon_1^{T} + f(t)\,\varepsilon_2^{T}, \quad (22.2)$$

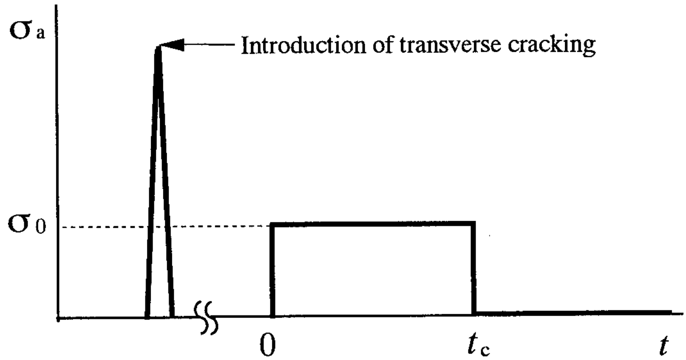

Figure 2. Stress history applied to $[0°/90°/-45°/+45°]_S$ specimens. The origin of time t is located at a starting point of creep loading.

where $\varepsilon_L^M(t)$ and $\varepsilon_L^T(t)$ denote the mechanical and thermal components, respectively. It is easily found that $\varepsilon_0(t)$ is the strain of a laminate without transverse cracks.

Now, we consider the strain response to the stress history depicted in Fig. 2. First a specimen is pre-loaded for introducing transverse cracking. Next, the stress given by the following equation is applied:

$$\sigma_a(t) = \begin{cases} \sigma_0 H(t) & (0 < t \leqslant t_c), \\ \sigma_0 H(t) - \sigma_0 H(t - t_c) & (t_c < t), \end{cases} \tag{23}$$

where $H(t)$ denotes a Heaviside's step function, and σ_0 and t_c are constant stress and duration of creep loading, respectively. Since the thermal (residual) strain reaches the steady-state value ε_L^R at sufficiently long time after generation of transverse cracking [6, 9], the corresponding strain is derived from equation (21) as

$$\varepsilon_L(t) = \begin{cases} \varepsilon_L^M(t) + \varepsilon_L^R & (0 < t \leqslant t_c), \\ \varepsilon_L^M(t) - \varepsilon_L^M(t - t_c) + \varepsilon_L^R & (t_c < t). \end{cases} \tag{24}$$

2.5. Relaxation moduli

It is assumed that the elastic moduli are expressed as the following functions:

$$E_k(t) = E_k^0\left(1 - e_k t^{n_k}\right), \tag{25.1}$$

$$G_k(t) = G_k^0\left(1 - g t^m\right), \tag{25.2}$$

where E_k^0, G_k^0, e_k, g, n_k and m are positive constants. Equation (25.1) with the use of equation (13) gives the Young's modulus of the laminate

$$E_0(t) = E_0^0\left(1 - \frac{E_1^0 e_1 t^{n_1} + E_2^0 e_2 t^{n_2} + 2E_3^0 e_3 t^{n_3}}{4E_0^0}\right), \tag{26}$$

with

$$E_0^0 = \frac{E_1^0 + E_2^0 + 2\,E_3^0}{4}. \tag{27}$$

Substituting equations (25.1), (25.2) and (26) into equations (19) and (20) using equations (A6) and (11), we obtain the Laplace transforms of $\varepsilon_0(t)$, $f(t)$ and $\alpha(t)$ for $0 < t \leqslant t_c$ as presented in Appendix 2.

First, the original functions of equations (A8) and (A9), namely, $\varepsilon_0(t)$ and $f(t)$ are calculated with the aid of a numerical Laplace transform method [5]. Then, the strain response of the laminate to the stress history expressed by equation (23) is calculated using equations (22.1) and (24).

3. EXPERIMENTAL

A unidirectional laminate, $[0°/90°]_{2S}$ cross-ply laminate and $[0°/90°/-45°/45°]_S$ quasi-isotropic laminate were fabricated by a filament winding technique. The final cured thickness was 2.0 mm for the unidirectional and cross-ply laminates and 3.6 mm for the quasi-isotropic laminate. The average fiber volume fraction was 0.62. Coupon specimens of [0°], [10°], [90°], $[\pm 45°]_{2S}$ and $[0°/90°/-45°/45°]_S$ were cut from the laminate plates. The aluminum tabs of length 50 mm were bonded on the specimens. The strain gages were adhesively bonded on the specimens to measure the strains. The loading tests were performed with an electrohydraulic testing machine at a room temperature. First, the $[0°/90°/-45°/45°]_S$ specimens were initially loaded so that transverse cracks were generated only in the transverse layers. The transverse crack density $1/2L$ was defined as the number of transverse cracks per unit length within 60 mm along the specimen length. Next, the creep and recovery tests for the [0°], [10°], [90°], $[\pm 45°]_{2S}$ and $[0°/90°/-45°/45°]_S$ ($1/2L =$ 0.00, 0.25 and 0.50/mm) specimens were performed. After constant load which corresponds to 0.25% tensile strain was applied for 10 hours, the specimens were unloaded and kept at zero load for 12 hours. It should be noted that neither new transverse cracks nor any other damage such as delamination initiate during the creep and recovery tests.

The relaxation moduli were determined through the following procedure. First, the creep compliance $S_1(t)$, $S_2(t)$ and $S_3(t)$ were measured from the creep tests of [0°], [90°] and $[\pm 45°]_{2S}$ specimens, respectively. Then, the relaxation moduli $E_1(t)$, $E_2(t)$ and $E_3(t)$ were calculated using the following relation:

$$E_k(t) = L^{-1}\left[\frac{1}{s^2 \hat{S}_k(s)}\right], \tag{28}$$

where L^{-1} denotes inverse Laplace transform. Similarly, the in-plane shear modulus $G_1(t)(G_{12}(t))$ was given by

$$G_1(t) = L^{-1}\left[\frac{1}{s^2 \hat{S}_6(s)}\right], \tag{29}$$

with

$$S_6(t) = \frac{S_x(t) - \cos^4 10° S_1(t) - \sin^4 10° S_2(t)}{\cos^2 10° \sin^2 10°} \tag{30}$$

where S_6 and S_x denote the in-plane shear creep compliance and creep compliance of a [10°] specimen, respectively. Other shear moduli $G_2(t)$and $G_3(t)$ are expressed by equation (25.2) when $G_k^0 (k = 1, 2, 3)$ are given.

4. RESULTS AND DISCUSSION

Figure 3 shows the normalized Young's moduli $E_1(t)$, $E_2(t)$, $E_3(t)$ and shear modulus $G_1(t)$ measured in the creep tests of the [0°], [90°], [±45°]$_{2S}$ and [10°] specimens, respectively. Pronounced time-dependence is observed in $E_2(t)$, $E_3(t)$and $G_1(t)$ whilst deformation in the fiber direction ($E_1(t)$) is almost time-independent.

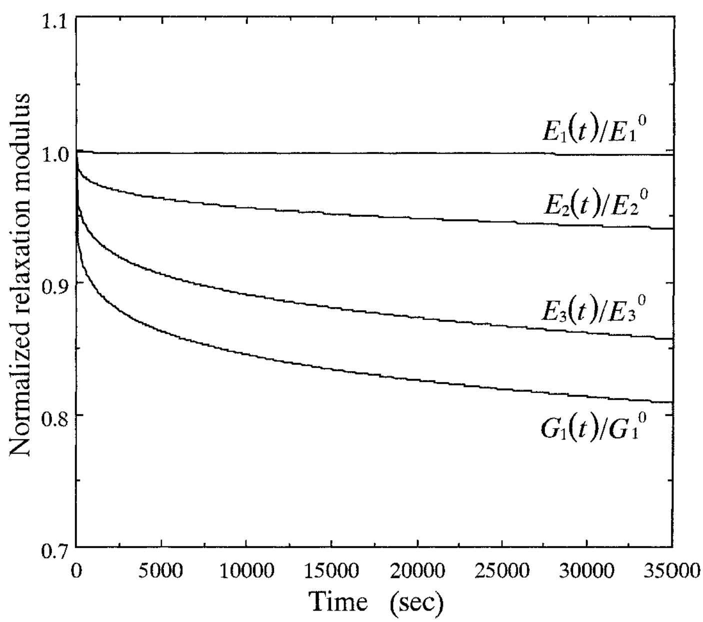

Figure 3. Normalized relaxation moduli $E_k(t)/E_k^0 (k = 1, 2, 3)$ and $G_1(t)/G_1^0$ obtained from creep tests of [0°], [90°], [±45°]$_{2S}$ and [10°] specimens.

Table 1.
Viscoelastic constants in equations (25.1) and (25.2)

E_1^0 (GPa)	E_2^0 (GPa)	E_3^0 (GPa)	G_1^0 (GPa)	G_2^0 (GPa)	G_3^0 (GPa)	e_1 ($\sec^{-n_1}$)
38.4	10.7	19.0	3.8	3.8	3.8	6.09×10^{-4}
e_2 ($\sec^{-n_2}$)	e_3 ($\sec^{-n_3}$)	g ($\sec^{-m}$)	n_1	n_2	n_3	m
4.37×10^{-3}	1.38×10^{-2}	2.87×10^{-2}	0.154	0.249	0.224	0.182

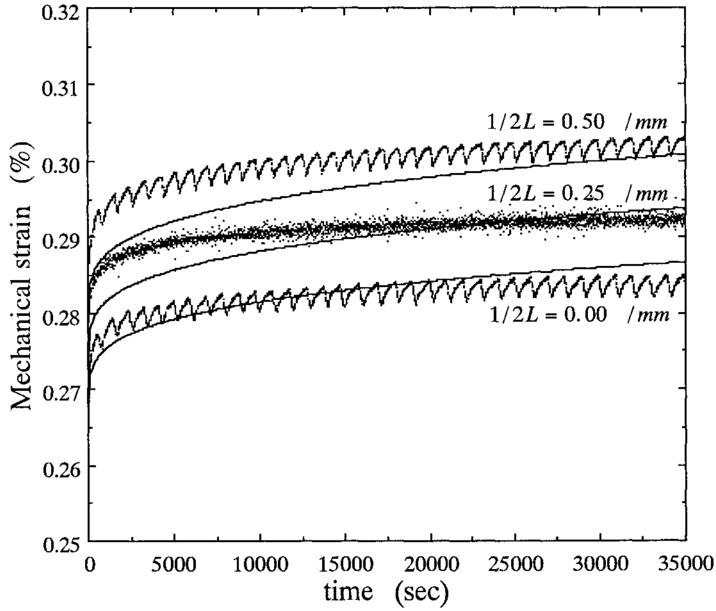

(a)

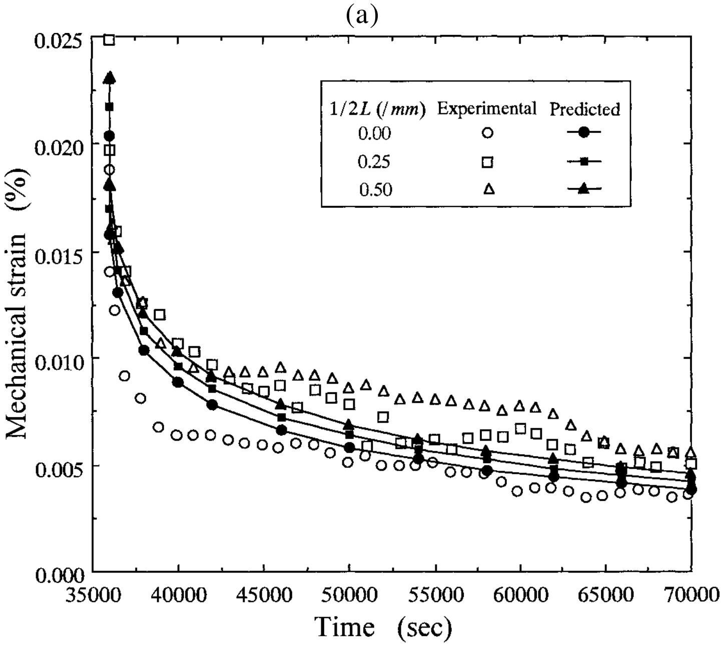

(b)

Figure 4. Mechanical strain response in (a) creep ($\sigma_0 = 58$ MPa) and (b) recovery tests of $[0°/90°/-45°/+45°]_S$ specimens for transverse crack density 0.00, 0.25 and 0.50/mm.

Viscoelastic constants of the lamina in equations (25.1) and (25.2) determined from the above creep curves are summarized in Table 1.

Figures 4a and b depict the mechanical strains during the creep ($\sigma_0 = 58$ MPa) and recovery tests of the $[0°/90°/-45°/45°]_S$ specimens for transverse crack density 0.00, 0.25 and 0.50/mm. It should be noticed that thermal strains are not included in the creep strains. Initial strain increases with increasing transverse crack density (Fig. 4a). However, evident difference in creep strain increment among the three curves can not be seen. This is because the change in $f(t)$ is relatively small compared with the increase in $\varepsilon_0(t)$. An increase in $f(t)$ depends on a decrease in the shear moduli $G_k(t)$. If the shear moduli decreases largely with time, effect of transverse crack density on creep strain increment is more evidently observed. With regard to recovery behavior (Fig. 4b), the residual strain increases with increasing transverse crack density although its difference is very small.

Predictions are also presented in Fig. 4 by solid lines. The viscoelastic properties of each lamina listed in Table 1 are employed in the calculation. Here we discuss only creep behavior (Fig. 4a) because it is difficult to compare the predicted recovery strain with the experimental one. Contradiction between experimental results and predictions is observed especially in the initial creep portion (Fig. 4a). One of the reasons for this contradiction is the relaxation moduli expressed by equations (25.1) and (25.2). However, the predicted creep strain increments during creep loading are 204, 218 and 230 $\mu\varepsilon$ for transverse crack density 0.00, 0.25 and 0.50/mm, respectively, which are comparable with the experimental results and thus the validity of the model is verified.

5. CONCLUSIONS

An analytical model was proposed for predicting creep and recovery behavior of a quasi-isotropic laminate with transverse cracking. The model predicts the creep and recovery strains of the laminate with the aid of viscoelastic constants measured in the creep tests of the constituent layers. The transverse and shear relaxation moduli show time-dependence and have an effect on creep behavior of a quasi-isotorpic laminate. Predictions are in reasonably good agreement with the experimental results.

Acknowledgements

Authors would like to express appreciation of technical support from Mr. Reg Whattingham of University of Surrey. Keiji Ogi is grateful to the Ministry of Education of Japan for providing an opportunity to study at University of Surrey.

REFERENCES

1. R. H. Moore and D. A. Dillard, Time-dependent matrix cracking in cross-ply laminates, *Composites Science and Technology* **39**, 1–12 (1990).

2. J. Raghavan and M. Meshii, Time-dependent damage in carbon fibre-reinforced polymer composites, *Composites Part A* **27**, 1223–1227 (1996).
3. K. Ogi and Y. Takao, Evolution of transverse cracking in CF/Epoxy cross-ply laminates under creep loading, *J. Reinf. Plast. Compos.* **13**, 220–230 (1999).
4. K. Ogi and Y. Takao, Modeling of time-dependent behavior of deformation and transverse cracking in cross-ply laminates, *Adv. Composite Mater.* **10**, 39–62 (2001).
5. K. Ogi and T. Shiraishi, Viscoelastic shear lag analysis of a cross-ply laminate with transverse cracking, in: *Proceedings of the 7th International Conference on Creep and Fatigue at Elevated Temperatures*, Tsukuba, pp. 277–280 (2001).
6. K. Ogi and P. A. Smith, Characterization of transverse cracking in a quasi-isotropic GFRP laminate under flexural loading, *Applied Composite Materials* (in press).
7. P. A. Smith and S. L. Ogin, On transverse matrix cracking in cross-ply laminates loaded in simple bending, *Composites Part A* **30**, 1003–1008 (1999).
8. J. -W. Lee and I. M. Daniel, Progressive transverse cracking of crossply composite laminates, *J. Compos. Mater.* **24**, 1225–1243 (1990).
9. F. Bassam, L. Boniface, K. Jones and S. L. Ogin, On the behavior of the residual strain produced by matrix cracking in cross-ply laminates, *Composites Part A* **29A**, 1425–1432 (1998).

APPENDIX 1. DERIVATION OF THE DIFFERENTIAL EQUATION (10)

Taking Laplace transforms of equations (1) to (3), the Laplace transforms of the shear stresses $\tau_{xz,k}$ are expressed as

$$\begin{aligned}
\hat{\tau}_{xz,1}(x,s) &= \begin{cases} 0 & (2a < z \leqslant 5a/2), \\ s\hat{G}_1(s)\big(2\hat{C}_1 z + \hat{C}_2\big) & (3a/2 < z \leqslant 2a), \end{cases} \\
\hat{\tau}_{xz,1}(x,s) &= s\hat{G}_2(s)\big(2\hat{C}_4 z + \hat{C}_5\big) \quad (a/2 < z \leqslant 3a/2), \\
\hat{\tau}_{xz,3}(x,s) &= \begin{cases} s\hat{G}_3(s)\big(2\,\hat{C}_7\, z + \hat{C}_8\big) & (0 < z \leqslant a/2), \\ 0 & (-3a/2 \leqslant z \leqslant 0), \end{cases}
\end{aligned} \tag{A1}$$

where a circumflex accent denotes a Laplace transform. Using the boundary conditions (7.1) to (7.6) together with equations (1), (5) and (A1), we obtain

$$\begin{aligned}
&\frac{\partial}{\partial x}\big(\hat{\bar{u}}_2(x,s) - \hat{\bar{u}}_1(x,s)\big) \\
&\quad = \frac{88\hat{G}_1(s)\hat{G}_2(s) + 80\hat{G}_2(s)\hat{G}_3(s) + 96\hat{G}_1(s)\hat{G}_3(s) + 55\{\hat{G}_2(s)\}^2}{24\hat{G}_2(s)(24\hat{G}_3(s) + 11\hat{G}_2(s))} \\
&\qquad \times\, a^2 \frac{\partial \hat{C}_1(x,s)}{\partial x},
\end{aligned} \tag{A2}$$

and

$$\hat{\tau}_1(x,s) = -as\hat{G}_1(s)\hat{C}_1(x,s), \tag{A3.1}$$

$$\hat{\tau}_2(x,s) = -as\hat{G}_3(s)\frac{24\hat{G}_1(s) + 10\hat{G}_2(s)}{24\hat{G}_3(s) + 11\hat{G}_2(s)}\hat{C}_1(x,s). \tag{A3.2}$$

Using equations (9.2), (A3.1) and (A3.2), we have

$$\frac{\partial^2 \hat{\sigma}_2(x,s)}{\partial x^2} = s\frac{11\hat{G}_1(s)\hat{G}_2(s) + 10\hat{G}_2(s)\hat{G}_3(s) + 48\hat{G}_1(s)\hat{G}_3(s)}{24\hat{G}_3(s) + 11\hat{G}_2(s)}\frac{\partial \hat{C}_1(x,s)}{\partial x}. \quad \text{(A4)}$$

Combination of equation (A2) with equation (A4) leads to

$$\frac{\partial^2 \hat{\sigma}_2(x,s)}{\partial x^2} = s\hat{H}(s)\left[\frac{\partial \hat{\bar{u}}_2(x,s)}{\partial x} - \frac{\partial \hat{\bar{u}}_1(x,s)}{\partial x}\right], \quad \text{(A5)}$$

with

$$\hat{H}(s) = \frac{24\hat{G}_2(s)}{a^2} \times \frac{11\hat{G}_1(s)\hat{G}_2(s) + 10\hat{G}_2(s)\hat{G}_3(s) + 48\hat{G}_1(s)\hat{G}_3(s)}{88\hat{G}_1(s)\hat{G}_2(s) + 80\hat{G}_2(s)\hat{G}_3(s) + 96\hat{G}_1(s)\hat{G}_3(s) + 55\left\{\hat{G}_2(s)\right\}^2}. \quad \text{(A6)}$$

On the other hand, equations (4) and (6) give the Laplace transform of the mechanical axial strain in each ply as

$$\frac{\partial \hat{\bar{u}}_k(x,s)}{\partial x} = \frac{\hat{\sigma}_k(x,s) - \hat{\sigma}_k(s)^{\mathrm{T}}}{s\hat{E}_k(s)}, \quad \text{(A7)}$$

where $\hat{\sigma}_k^{\mathrm{T}}(s) = \hat{E}_k(s)\,\varepsilon_k^{\mathrm{T}}$. By using equations (5) and (8), substitution of equation (A7) into equation (A5) yields equation (10).

APPENDIX 2. LAPLACE TRANSFORMS OF $\varepsilon_0.t/$, $f\ .t/$ AND $\alpha.t/$

$$\hat{\varepsilon}_0(s) = \frac{\sigma_0}{sE_0^0\left\{1 - \frac{1}{4}\left(\frac{b_1}{s^{n_1}} + \frac{b_2}{s^{n_2}} + \frac{2b_3}{s^{n_3}}\right)\right\}}, \quad \text{(A8)}$$

$$\hat{f}(s) = f_0\frac{\tanh(\hat{\alpha}(s)L)}{s\tanh(\alpha_0 L)} \times \sqrt{\frac{\left(1 - \frac{E_0^0}{E_2^0}\frac{b_2}{s^{n_2}}\right)^3}{\left\{1 - \frac{E_0^0}{E_1^0 + 2E_3^0}\left(\frac{b_1}{s^{n_1}} + \frac{2b_3}{s^{n_3}}\right)\right\}\left\{1 - \frac{1}{4}\left(\frac{b_1}{s^{n_1}} + \frac{b_2}{s^{n_2}} + \frac{2b_3}{s^{n_3}}\right)\right\}\left(1 - \frac{c}{s^m}\right)}}, \quad \text{(A9)}$$

$$\hat{\alpha}(s) = \alpha_0 \sqrt{\frac{\left\{1 - \frac{1}{4}\left(\frac{b_1}{s^{n_1}} + \frac{b_2}{s^{n_2}} + \frac{2b_3}{s^{n_3}}\right)\right\}\left(1 - \frac{c}{s^m}\right)}{\left(1 - \frac{E_0^0}{E_2^0}\frac{b_2}{s^{n_2}}\right)\left\{1 - \frac{E_0^0}{E_1^0 + 2E_3^0}\left(\frac{b_1}{s^{n_1}} + \frac{2b_3}{s^{n_3}}\right)\right\}}}, \quad \text{(A10)}$$

with

$$b_k = \frac{E_k^0 e_k \Gamma(n_k + 1)}{E_0^0} \quad (k = 1, 2, 3), \quad \text{(A11)}$$

$$c = g\Gamma(m + 1), \quad \text{(A12)}$$

$$f_0 = \frac{E_2^0}{E_1^0 + 2E_3^0} \frac{\tanh(\alpha_0 L)}{\alpha_0 L}, \quad \text{(A13)}$$

$$\alpha_0 = \sqrt{\frac{96 E_0^0 G_2^0}{a^2 E_2^0 \left(E_1^0 + 2E_3^0\right)} \frac{11 G_1^0 G_2^0 + 10 G_2^0 G_3^0 + 48 G_1^0 G_3^0}{88 G_1^0 G_2^0 + 80 G_2^0 G_3^0 + 96 G_1^0 G_3^0 + 55\left(G_2^0\right)^2}}, \quad \text{(A14)}$$

where Γ denotes the Gamma function.